Liquid-phase Hydrogenation of Nitrobenzene in a Slurry Reactor

Flüssigphasenhydrierung von Nitrobenzen im Rührreaktor mit suspendiertem Katalysator

FRITZ TUREK, RAINER GEIKE and RÜDIGER LANGE

Technical University "Carl Schorlemmer" Leuna-Merseburg, 42 Merseburg (G.D.R.)

(Received October 4, 1985)

Abstract

This article deals with studies of the liquid-phase hydrogenation of nitrobenzene to aniline in a discontinuous laboratory-scale stirred reactor with suspended Ni catalyst. The influence of temperature, pressure, nitrobenzene concentration and pH value on the reaction rate was investigated. Apart from the kinetics, a series of technically relevant effects which are not covered by the kinetic model are studied.

A rate equation of the Langmuir–Hinshelwood type was selected on the basis of the reaction scheme and the experimental data. The kinetic model was examined by checking with the experimental data in an agitated reactor and in an industrial reactor.

Kurzfassung

Für die Flüssigphasenhydrierung von Nitrobenzen zu Anilin werden experimentelle Untersuchungen zum Prozessablauf vorgestellt. Neben der Ermittlung des kinetischen Modells wird eine Reihe technisch relevanter Einflussgrössen, die durch das kinetische Modell nicht erfasst werden, untersucht. Dazu gehören die Katalysatoraktivierung, die Katalysatorkorngrössenveränderung, der Einfluss des pH-Wertes und die Nebenproduktbildung.

Die Ergebnisse demonstrieren quantitativ und qualitativ die Vielfalt der zu bearbeitenden Probleme bei technisch orientierten Aufgabenstellungen.

Synopse

Bei der Berechnung, Optimierung und Beurteilung des Betriebsverhaltens technischer Gas–Flüssig–Feststoff-Reaktoren spielt die Reaktionskinetik gewöhnlich eine zentrale Rolle. Neben der Reaktionskinetik treten weitere technisch und versuchstechnisch relevante Teilprozesse und Einflussfaktoren auf, die durch die Prozesskinetik nicht oder nur schwer erfassbar sind und zu denen häufig nur qualitative Aussagen gewinnbar sind.

Am Beispiel der Flüssigphasenhydrierung von Nitrobenzen werden im folgenden neben der Ermittlung der Reaktionskinetik experimentelle Ergebnisse zum Einfluss weiterer Faktoren auf den Prozessablauf mitgeteilt. Die Versuche zur Ermittlung der Reaktionskinetik wurden im Laborrührautoklaven durchgeführt (Bild 1). Als Mass für die Reaktionsgeschwindigkeit der Hydrierung wird die Abnahme des Wasserstoffpartialdruckes im geschlossenen System der Versuchsapparatur verwendet. Die gemessenen Konzentration–Zeit-Verläufe zeigen jeweils einen weiten linearen Bereich (Bild 2).

Die experimentellen Ergebnisse der Reaktionskinetik lassen sich gut mit einem Langmuir–Hinshelwood-Ansatz beschreiben (Gln. (2)–(4)). Die Nachrechnung von experimentellen Daten ist auf Bild 3 dargestellt. Zur Überprüfung der Eignung des kinetischen Modells wurden experimentelle Werte, die mit einem Schüttelreaktor erhalten worden sind, in die Betrachtungen einbezogen (Bild 4). Unter dem Gesichtspunkt der Nutzung der Ergebnisse für die Prozessanalyse und die mathematische Beschreibung eines technischen Reaktors erfolgten Untersuchungen zur Anilinausbeute (Gl. (5), Bild 5), zum Einfluss der Katalysatoraktivierung (Bild 6), zum Einfluss des pH-Wertes (Bild 7), zur Wasserstofflöslichkeit (Bild 11), zur Kopplung von Stofftransport und Reaktion (Bilder 8 und 9) und zur Katalysatorkorngrössenveränderung (Bild 13). Die Aussagen zum Einfluss der Stofftransportprozesse auf den Reaktionsablauf sind sowohl für die Bewertung der reaktionskinetischen Experimente, als auch für das mathematische Modell des technischen Reaktors von Bedeutung. Es zeigt sich, dass bei sehr kleinen Konzentrationen der Flüssigkomponenten auch diesbezügliche Stofftransporthemmungen signifikant werden können (Bild 9).

Die Katalysatorzerkleinerung infolge der Rührbeanspruchung wirkt sich einmal beschleunigend auf

die inneren und äusseren Stofftransportprozesse aus und zum anderen kann bei sehr kleinen Partikelgrössen die Katalysatorabtrennung problematisch werden (Bild 12).

Schlussfolgernd aus den Ergebnissen kann eingeschätzt werden, dass für eine Massstabsübertragung die Einbeziehung der Reaktionskinetik und der Stofftransportprozesse in das mathematische Modell eines technischen Rührreaktors sinnvoll ist und die weiteren Effekte und Einflussgrössen als eingrenzende Rahmenbedingungen qualitativ und quantitativ in die Auslegung bzw. Prozessgestaltung einbezogen werden.

Introduction

The reaction kinetics play a decisive role in the calculation, optimization and evaluation of the operational behaviour of industrial gas–liquid–solid reactors. Laboratory-scale stirred tank reactors with suspended catalyst were shown to be useful for the experimental determination of the kinetics in these three-phase catalytic reactions.

A state of quasi-homogeneous mixing and a high mass transfer rate is obtained with sufficiently small catalyst particles and high turbulence in the liquid phase, which can be reached by an appropriate stirrer shape and flow breakers [1–4].

Apart from the reaction kinetics, there are certain single processes and factors which are of importance in large-scale and laboratory-scale operation, but cannot be covered adequately, or not at all, by process kinetics, and often only yield qualitative data. In catalytic gas–liquid–solid reactions, such processes and factors include catalyst activation and catalyst abrasion, the effect of the pH value, and the occurrence of side reactions.

Whereas a great number of papers reporting qualitative and quantitative data are available for reaction kinetics, internal and external mass transfer, and the hydrodynamics of definite operational conditions, information about the factors mentioned above is scarce and often incomplete [3–8]. In the following, the reaction kinetics is determined, and experimental results concerning the effects of further factors on the global process are reported.

Experimental conditions and results

The experiments for determining the reaction kinetics were carried out in a discontinuous laboratory-scale stirred autoclave with the following parameters:

Liquid volume	0.5–1.0 l
Catalyst	Ni/Al_2O_3
Catalyst loading	0.5–1.0 g
Catalyst particle size	20–40 μm
Reaction temperature	50–150 °C
Pressure	0.2–2.0 MPa
Initial concentration of nitrobenzene	4.3×10^{-3}–4.3×10^{-2} mol l^{-1}
Solvent	ethanol
Liquid-phase composition (except nitrobenzene)	$y_{AN} = 0.5$ $y_{H_2O} = 0.2$ $y_{ET} = 0.3$

The drop of hydrogen partial pressure in the closed system of the experimental apparatus was used as a measure of the reaction rate of hydrogenation. This method considerably reduces the expense of the experiment and can also be applied to relatively fast reactions. The method was checked in several experiments by determining the change of the nitrobenzene concentration with the help of gas chromatography. The average deviation of the results obtained by these two methods was less than 5%. A schema of the experimental apparatus is shown in Fig. 1. The change of pressure can be followed using a differential pressure meter (8) inserted between the comparative tank (9) at constant pressure and the reactor during the experiments. At the beginning of each experiment, the nitrobenzene (dissolved in 50 ml of the reaction mixture) was fed in through a pressure compensation tank. The resulting gas and liquid volume changes were taken into account in the evaluation of the measured data.

A reproducibility test revealed that the catalyst activity decreased. After approximately 25 hours of operation, a region is reached of relatively small activity change, the level of activity being about one-third of the initial activity. The reaction kinetics was determined within the region of small activity drop, which was corrected with the help of an activity coefficient. For

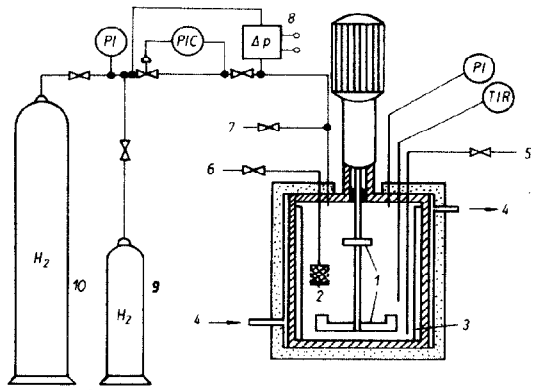

Fig. 1. Experimental set-up: 1, stirrer blade; 2, filter; 3, stream splitter; 4, constant temperature bath; 5, liquid outlet; 6, sampling tube; 7, inlet for mixture; 8, $\Delta p/\Delta t$ measurement; 9, compensation tank; 10, pressurized hydrogen container.

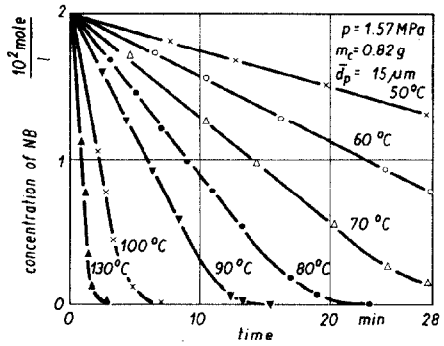

Fig. 2. Effect of temperature on the concentration–time curves of nitrobenzene.

this purpose, a comparative test was carried out after each experimental series. Figure 2 shows the concentration–time curves measured as a function of temperature. A linear curve is obtained up to the region of low concentration. From this it follows that the reaction is of zero order with respect to nitrobenzene, which is confirmed by the results reported in refs. 9 and 10.

The discontinuity in the curves at low concentration can be explained by changes in the apparent order of reaction according to eqn. (3).

Reaction kinetics

The hydrogenation of nitrobenzene to aniline proceeds according to the following reaction scheme:

$$\bigcirc\!\!-NO_2 + 3H_2 \longrightarrow \bigcirc\!\!-NH_2 + 2H_2O \qquad (1)$$

via the intermediate stages of nitrobenzene and phenylhydroxylamine. On the basis of physically and chemically well-founded assumptions with respect to the reaction mechanism [9–11], the following reaction rate can be derived:

$$r = kK_{NB}c_{NB}K_{H_2}c_{H_2}(1 + K_{NB}c_{NB} + K_{AN}c_{AN} + K_{ET}c_{ET} + K_{H_2O}c_{H_2O})^{-1}(1 + K_{H_2}c_{H_2})^{-1} \qquad (2)$$

In accordance with the technological aim of the experiments, they did not involve variations of c_{AN}, c_{ET} and c_{H_2O}. Hence these concentrations were only subject to very slight changes resulting from the reaction scheme (1). They were not taken into consideration in the evaluation of the experiments, and the following simplified reaction equation is obtained:

$$r = \frac{kK_{NB}c_{NB}}{1 + K_{NB}c_{NB}} f(p_{H_2}) \qquad (3)$$

where

$$c_{H_2} = c^*_{H_2} \qquad (4)$$

$$f(p_{H_2}) = \frac{K_{H_2}\alpha_{H_2}p_{H_2}}{(1 + K_{H_2}\alpha_{H_2}p_{H_2})}$$

(Hence k and K_{NB} also cover the potential effects of adsorption inhibition of components AN, ET and H_2O.)

The parameters k, K_{NB} and K_{H_2} are determined by adapting the model constants of the material balance of the laboratory reactor used (eqn. (5)) to the measured data.

$$dc_{NB}/dt = -rc_k \qquad (5)$$

First the parameters k and K_{H_2} are determined from the linear sections of the concentration–time curves.

$$k = 4.128 \times 10^6 \frac{\text{mol}}{\text{kg s}} \exp\left(-\frac{53.25 \text{ kJ mol}^{-1}}{RT}\right)$$

$$K_{H_2} = 1.097 \times 10^{-2} \text{ mol}^{-1} \exp\left(\frac{28.29 \text{ kJ mol}^{-1}}{RT}\right)$$

K_{NB} of these values can be determined on the basis of the fact that the curvature of the concentration–time curve is caused by the inhibition of the NB adsorption alone.

$$K_{NB} = 3.503 \times 10^{14} \text{ mol}^{-1} \exp\left(-\frac{71.7 \text{ kJ mol}^{-1}}{RT}\right)$$

The temperature dependence of K_{NB} is positive, contrary to the theoretical assumptions. This problem has not been investigated in the present work, the purpose of which was to establish a practical mathematical model for the scale-up. This effect could presumably be explained as follows. In regions of very small nitrobenzene concentration, the adsorption term of aniline ($K_{AN}c_{AN}$), which has not been taken into consideration in the model, also becomes significant. This results in a positive apparent temperature dependence of K_{NB}.

It was proved that mass transfer inhibition did not cause significant error in the kinetic parameters determined [11]. Major inhibitions in mass transfer only occur at the highest temperature ($T = 130$ °C) (see also Fig. 9). A comparison of experimental and predicted reaction rates (eqn. (3)) is shown in Fig. 3. The experimental data for r were obtained from the linear regions of the c_{NB}–t curves measured.

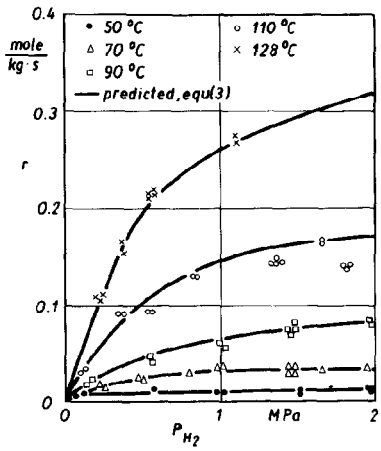

Fig. 3. Comparison of experimental and predicted reaction rates.

Test of the kinetic model

The model was tested for adaptibility using the experimental data from a laboratory-scale agitated reactor under different experimental conditions ($V_Q = 0.1$ l, $T = 9$–45 °C, $p = 0.11$ MPa). Comparison of the temperature dependence is presented in Fig. 4.

The measured data of the laboratory agitated reactor were converted with the help of eqns. (3) and (4), because the pressures in the laboratory stirred reactor differed from those in the agitated reactor.

In addition, values of the reaction rate for a catalyst sample taken from an industrial stirred tank reactor were plotted (Fig. 4).

Deviations between the two variants are primarily due to partially different catalyst activities and are within the range of possible errors in measurement.

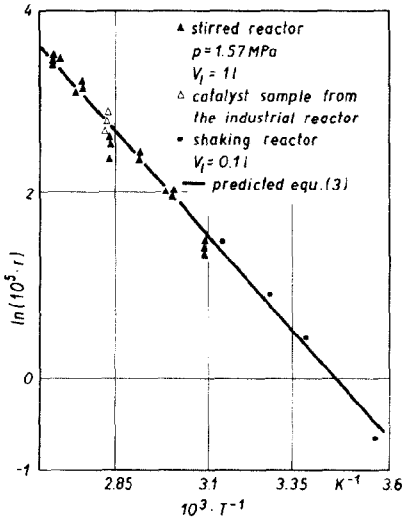

Fig. 4. Test of the kinetic model.

Aniline yield

It is known from other publications [12, 13] that side reactions in nitrobenzene hydrogenation mainly start from aniline. In the present case, the following by-products were quantitatively detected by gas chromatography: cyclohexanol, *N*-ethyl aniline, toluidine, cyclohexyl amine, and diaminobenzene, of which only cyclohexanol and *N*-ethyl aniline were formed in technologically relevant amounts.

For these two components, the temperature dependence of the rate of formation was determined to be

$$R_{CH} = 3.94 \times 10^{10} \exp\left(-\frac{71.2}{RT}\right) \quad \text{mol kg}^{-1}\,\text{s}^{-1}$$

$$R_{EAN} = 4.44 \times 10^{9} \exp\left(-\frac{92.5}{RT}\right) \quad \text{mol kg}^{-1}\,\text{s}^{-1}$$

No significant dependence of the above reaction rates on p_{H_2} and c_{NB} could be detected.

With the help of this rate of by-product formation, a yield factor

$$f_y = 1 - \frac{R_{CH} + R_{EAN}}{R_{NB}} \qquad (6)$$

can be defined, which may be used for describing the aniline yield in the mathematical model of the process. The temperature dependence of the yield factor determined on the basis of the experimental data is represented in Fig. 5.

Effect of catalyst activation

It is a well-known fact that the conditions of activation are known to have a definite effect on the activity and mechanical strength of the catalyst. In the reduction of the nickel catalyst for hydrogenation reactions, the

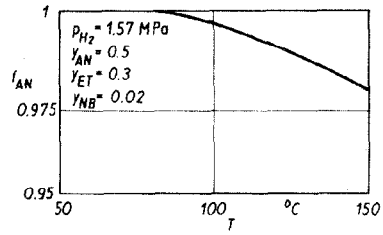

Fig. 5. Temperature dependence of the aniline yield.

following parameters are of importance: reduction temperature, reduction time, catalyst particle size, and hydrogen flow rate.

Combination of these factors yields an activity algorithm whose optimal values, as a rule, are specific to each reaction and each catalyst [14–16]. For instance, in ref. 14, the optimal reduction temperature (maximum activity of the catalyst) is stated to be 250 °C in nitrobenzene hydrogenation on the Ni catalyst and 400 °C in the hydrogenation of maleic acid butyl ester. In ref. 15, the maximum activity of an Ni/SiO_2 catalyst is reached at a reduction temperature of 400 °C. The effect of the reduction temperature in the present experiments is shown in Fig. 6.

Within the region investigated, a linear interdependence is found to exist between catalyst activity and reduction temperature. Obviously, the expected activity maximum only occurs outside the range of temperature studied. The effect of the reduction time on the catalyst activity is limited to the region of short reduction times ($t < 2$ h).

This statement roughly agrees with the results reported in ref. 14, that the equilibrium of reduction occurs after 1–1.5 h.

Effect of the pH value

In several publications, explanations are given of the effect of the pH value on the reaction rate and selectivity [14, 17, 18]. This effect is thought to be due to changes in the reaction mechanism or catalyst activity. Without

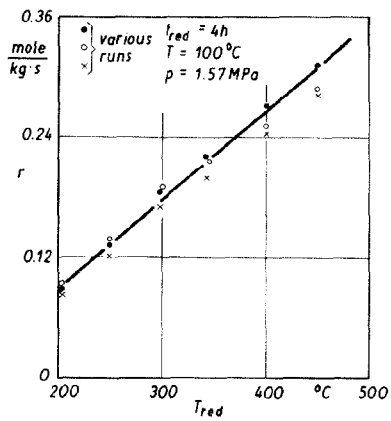

Fig. 6. Effect of the reduction temperature on the measured reaction rate.

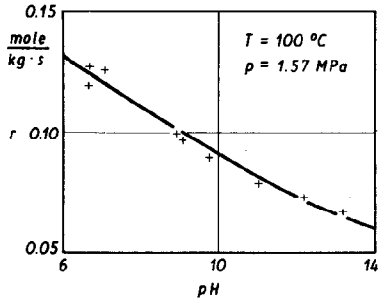

Fig. 7. Effect of pH value on the reaction rate.

a definite influence being exerted on the pH value of the present reaction, this value was always obtained to be around 9.5. The reaction kinetics was determined for this value. The pH values could be varied within a range 6.2–12.7 by adding KCl/KOH or KCl/HCl. The effect of these changes of the pH value on the reaction rate is represented in Fig. 7. Their application in industry has to be discussed from a technological and economic point of view.

Mass transfer and chemical reaction

In kinetic investigations of hydrogenation reactions in suspension reactors, it is necessary to analyse not only the reaction kinetics but also the mass transfer steps of gas to liquid for hydrogen, and liquid to catalyst, as well as pore diffusivity of hydrogen and substrate components. The stirring speed is an essential factor in the external mass transfer processes ($(ka)_{g,l}$ and $(ka)_{l,s}$). Figure 8 represents these mass transfer coefficients for the laboratory reactor used, plotted against the rotary speed of the stirrer. The course of $(ka)_{g,l}$ was measured with the help of H_2 absorption. Only one measured point being available for E_d, the curve was extrapolated with the correlation $E_d \propto n^3$. The values for $(ka)_{l,s}$ were calculated with the equations of Liepe and Möckel [19].

A strong effect of the rotary speed on $(ka)_{g,l}$ and a small effect on $(ka)_{l,s}$ is evident.

As regards the comparability of different reactor and stirrer shapes, it appears useful also to consider the correlation between the mass transfer parameters and the dissipation energy. In most papers covering these problems, only the effects of mass transfer as related to

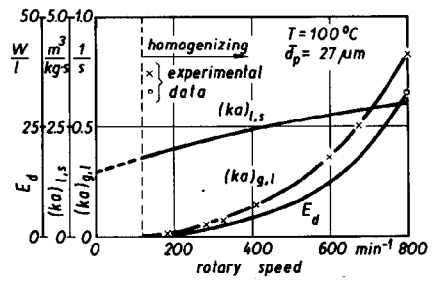

Fig. 8. Dependence of the rotary speed on the mass transfer effects.

hydrogen are analysed [1, 6, 7]. This procedure will generally be justified in cases of relatively large substrate concentrations and low pressures. For very small substrate concentrations, such as occur in processes aimed at complete conversion in stirred tank reactors, mass transfer inhibition may become dominant with respect to the substrate components.

In Fig. 9 the liquid to catalyst mass transfer and the effectiveness factor are demonstrated in dependence on c_{NB}.

The inhibition of liquid–solid mass transfer was calculated with

$$\frac{c_{NB,l} - c_{NB,k}}{c_{NB,l}} = \frac{r\eta_p}{(ka)_{l,s} c_{NB,l}} \tag{7}$$

η_p was determined on the basis of the correlation

$$\eta_p = f(\Phi, K_{NB} c_{NB}) \tag{8}$$

represented in Fig. 10.

Hydrogen solubility

A knowledge of the hydrogen solubility is of importance in the evaluation of mass transfer inhibition and the separation of the kinetic constants in eqn. (3). The solubility of hydrogen in the liquid mixture was also determined with the help of the experimental apparatus represented in Fig. 1.

The solubility coefficients determined for various liquid compositions in the temperature range 15–150 °C are summarized in Fig. 11.

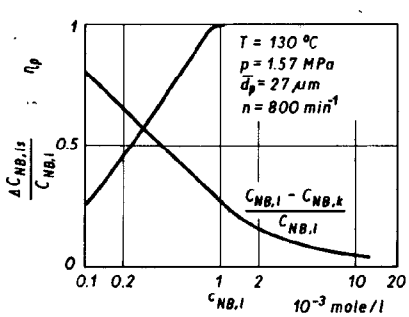

Fig. 9. Effect of nitrobenzene concentration on the mass transfer inhibitions.

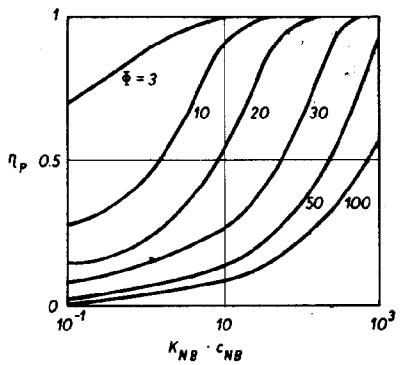

Fig. 10. Plot of η_p vs. $K_{NB}c_{NB}$.

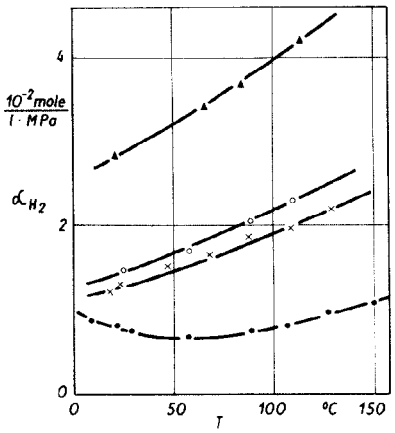

Fig. 11. Hydrogen solubility: ▲, 95% ET; ×, 50% AN, 30% ET, 20% H_2O; •, H_2O; ○, 40% An, 40% ET, 20% H_2O.

Catalyst particle size changes

As a consequence of the effect of stirring, the size of the catalyst particles decreases considerably, particularly with relatively large particle sizes. In the reaction process considered here, however, the catalyst particle size is a significant factor. Whereas decreasing particle size reduces internal and external mass transfer inhibition, very small particles involve problems with respect to catalyst separation from the liquid. The correlation which has been found to exist between the rate of formation of nitrobenzene and the particle size, as well as between the relative degree of separation in the sedimentation and the particle size, is represented in Fig. 12.

The separation curve is based on sedimentation analyses and represents the rate of separation for the particle size used, with the mean value $\bar{d}_p$. The reaction rate curve was calculated taking into consideration the liquid–catalyst mass transfer and the pore diffusion at very small c_{NB} values (see Fig. 9).

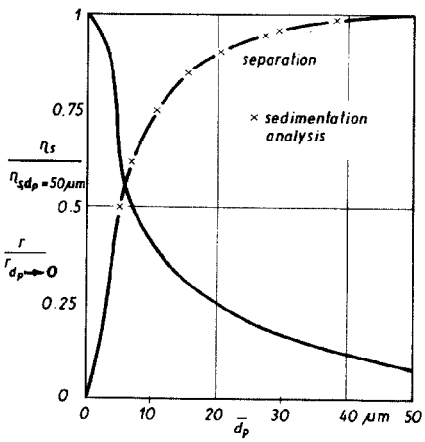

Fig. 12. Catalyst sedimentation and reaction rate as a function of particle size.

In the present case, catalyst crushing during the stirring process under reaction conditions was investigated in a laboratory stirred tank reactor. The catalyst, having a defined initial particle size, was added before the stirrer was started. Samples were taken at fixed stirring times t_{st} for an analysis of the particle size (sedimentation analysis and wet screening). Figure 13 demonstrates the measured temporal change of the average particle size.

An important fact in the utilization of the results is that after a certain stirring time the particle size remains relatively constant. Calculation of the reactor and separation of catalyst have to be related to this particle size. In cases of short times of catalyst utilization, the function $d_p = f(t_{st})$ can be used directly. Catalyst research faces the task of developing mechanically stable suspension catalysts, which will make a major contribution to certainty in the modelling of the reactor as well as in the separation of the catalyst.

It can be concluded from these results that the inclusion of reaction kinetics and the mass transfer processes in the mathematical model of an industrial stirred tank reactor will be useful for the scale-up and will qualitatively and quantitatively include other effects influencing the process in the design, or the formation of the processes, as limiting conditions.

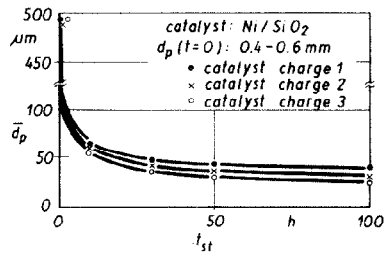

Fig. 13. Decrease of particle size.

Conclusions

Experimental investigations into the reaction kinetics of the liquid-phase hydrogenation of nitrobenzene to aniline have been presented. Apart from the determination of the kinetic model, a series of technologically relevant factors which are not covered by the kinetic model were studied.

The results quantitatively and qualitatively demonstrate the multiplicity of the problems to be treated in the design of industrial reactors from laboratory data.

Nomenclature

a	interface, m^{-1}
c_j	concentration of component, mol l^{-1}
d_p	particle size, m
E_d	dissipation energy, W l^{-1}
$(ka)_{g,l}$	gas–liquid mass transfer, s^{-1}
$(ka)_{l,s}$	liquid–solid mass transfer, $m^3\ kg^{-1}\ s^{-1}$
k	reaction rate constant, mol $kg^{-1}\ s^{-1}$

K	adsorption equilibrium constant, $l\ mol^{-1}$
m	mass, g
n	rotary speed, min^{-1}
p	pressure, MPa
r	reaction rate, $mol\ kg^{-1}\ s^{-1}$
R	gas constant, $J\ mol^{-1}\ K^{-1}$
t	time, min
T	temperature, °C
V	volume, l
y	liquid-phase composition
α	solubility coefficient, $mol\ l^{-1}$ MPa
η	pore efficiency
Φ	Thiele modulus

Subscripts

AN	aniline
CH	cyclohexanol
EAN	ethyl aniline
ET	ethanol
NB	nitrobenzene
g	gas
k	catalyst
ℓ	liquid
s	solid

References

1 C. N. Satterfield, *Mass Transfer in Heterogeneous Catalysis*, MIT Press, Cambridge, MA, and London, 1970.

2 F. Turek, R. Geike, R. Lange and J. Hanika, *Chem. Tech. (Leipzig), 38* (1986) 54.

3 R. V. Chaudhari and P. A. Ramachandran, *AIChE J., 26* (1980) 177.

4 T. Bühlmann, *Dissertation*, ETH, Zurich, 1982.

5 V. R. Choudhary and S. K. Chauhari, *J. Chem. Tech. Biotechnol., 33A* (1983) 266.

6 D. J. Collins, A. D. Smith and B. H. Davis, *Ind. Eng. Chem., Prod. Res. Dev., 21* (1982) 279.

7 O. M. Kut, T. Bühlmann, F. Meyer and G. Gut, *Ind. Eng. Chem., Process Des. Dev., 23* (1984) 335.

8 P. B. Kalautri and S. B. Chandalla, *Ind. Eng. Chem., Process Des. Dev., 21* (1982) 186.

9 M. Mejstrikova, *Collect. Czech. Chem. Commun., 39* (1974) 2740.

10 V. Ruzicka and H. Snatrochova, *Collect. Czech. Chem. Commun., 34* (1969) 2999.

11 F. Turek and R. Geike, *Chem. Tech. (Leipzig), 33* (1981) 24.

12 J. Pasek, J. Tyrpekl and M. Machova, *Collect. Czech. Chem. Commun., 31* (1966) 4108.

13 V. M. H. Govindarao and K. V. R. Murthy, *J. Appl. Chem. Biotechnol., 25* (1975) 169.

14 K. Kolomaznik, V. Ruzicka, J. Soukup and V. Zapletal, *Collect. Czech. Chem. Commun., 33* (1968) 2449.

15 S. P. Noskova, M. S. Borisova and V. A. Dzisko, *Kinet. Katal., 16* (1975) 497.

16 J. Hanika, K. Sporka, V. Ruzicka and J. Bauer, *Collect. Czech. Chem. Commun., 44* (1979) 2619.

17 A. B. Finkeljstein, S. M. Kusmina and M. C. Morosova, *Kinet. Katal., 19* (1978) 236.

18 L. Cerveny and V. Ruzicka, *Catal. Rev. Sci. Eng., 24* (1982) 503.

19 F. Liepe and H.-O. Möckel, *Chem. Tech. (Leipzig), 28* (1976) 205.